International Journal on Interactive Design and Manufacturing (IJIDeM) (2018) 12:1423–1433
https://doi.org/10.1007/s12008-017-0452-6

TECHNICAL PAPER

Improvement of a knock model for natural gas SI engines through heat transfer evaluation

Andrés Felipe Sierra Parra[1] · **Adalberto Gabriel Díaz Torres**[1]

Received: 26 July 2017 / Accepted: 11 December 2017 / Published online: 21 December 2017

Abstract

Knock is an abnormal combustion phenomena capable of causing serious damage to spark ignition engines, and is a constraint to reach the maximum potential of the engine, since strategies to increase power output and improve efficiency such as turbocharging, increased compression ratio and the advancement of spark timing, also increase the possibility of knock occurrence. Therefore, it is crucial to take into account the limits imposed by knock in the design and operating conditions of the engine when using an engine computational model. In this article a zero-dimensional two-zone engine model, coupled with a chemical kinetic model for knock detection through end-gas auto-ignition is developed and validated, for a natural gas engine. Given the importance of an accurate knock prediction, five heat transfer coefficient correlations are compared to find the most suitable to predict the knock occurrence, through calculation of a knock criterion. Correlations from Sitkei and Annand were the most suitable to predict this knock criterion for the experimental data used, and the Sitkei correlation was later tested in a parametric study to predict the effect of spark timing, compression ratio, equivalence ratio and inlet temperature in knock occurrence and intensity. Results were in accordance with real engine behaviour when knock occurs.

Keywords Zero-D model · Engine knock model · Natural gas · Detailed kinetics · SI engine · Heat transfer correlation

List of symbols

A_R	Flow area of the valve (m^2)
A_s	Heat transfer area (m)
B	Cylinder bore (m)
C_D	Discharge coefficient
CR	Compression ratio
c_p	Specific heat capacity at constant pressure (J/kg K)
c_v	Specific heat capacity at constant volume (J/kg K)
D_V	Valve diameter (m)
dQ	Gas-wall heat transfer (J/CAD)
dQ_{chem}	Rate of energy released in combustion reactions (J/CAD)
h	Specific Enthalpy (J/kg)
h_g	Gas-wall heat transfer coefficient (W/m^2 K)
k_g	Thermal conductivity (W/m K)
L	Connecting rod length (m)
$l_{v,max}$	Maximum valve lift (m)
m	Mass of the gas (kg)
rpm	Engine rotational speed (rpm)
p	Cylinder gas pressure (Pa)
R	Specific gas constant (J/kg K)
S	Cylinder stroke length (m)
s_L	Laminar flame speed (m/s)
s_p	Averaged piston speed (m/s)
ST	Spark timing before top center (CAD)
T	Temperature (K)
T_w	Wall temperature (K)
u	Internal energy (J/kg)
V	Cylinder volume (m^3)
V_c	Cylinder clearance volume (m^3)
V_d	Cylinder swept volume (m^3)
x_b	Burned gas mass fraction
γ	Specific heat capacities ratio
μ	Dynamic viscosity (Pa s)
ϕ	Equivalence ratio
ρ	Density (kg/m^3)
τ	Auto-ignition delay (CAD)

✉ Andrés Felipe Sierra Parra
asierrap@eafit.edu.co; cepfelo@gmail.com

Adalberto Gabriel Díaz Torres
gdiaz@eafit.edu.co

[1] IEXS Group, Escuela de Ingeniería, EAFIT University, Carrera 49 # 7 Sur-50, Medellín, Colombia

θ	Crank angle (CAD)
θ_{knock}	Knock onset (CAD)

Subscripts

b	Burned
in	Intake
mot	Motoring
st	At spark timing
u	Unburned
w	Wall

Abbreviations

AFR	Air–fuel ratio
CAD	Crank angle degree
EVO	Exhaust valve open (CAD)
EVC	Exhaust valve close (CAD)
IVO	Inlet valve open (CAD)
IVC	Inlet valve close (CAD)
LHV	Lower heating value of the fuel (J/kg)

1 Introduction

Spark ignition (SI) engines have been the main power source for automobiles and other transport vehicles, due to their versatility, as SI engines can operate in a wide range of conditions using different fuels, and, despite SI engines use is increasingly restricted because of the need to slow down the global warning, it is expected to remain relevant for at least the next 20 years [1].

The regulation of engine pollutant emissions and the depletion of petroleum resources have boosted the shift of gasoline to alternative fuels, such as natural gas, which has gained a lot of attention in the last decades due to its potential to achieve lower pollutant emissions [2], higher thermal efficiency [3] and lower cost [4] in SI engines. Despite its lower energy content, natural gas has a higher octane number than gasoline, and hence a natural gas engine can use turbocharging and a higher compression ratio to increase power output or improve efficiency, and can therefore, be a suitable replacement for gasoline as fuel in SI engines.

To improve natural gas engine performance in terms of energetic efficiency, fuel economy and pollutant emissions [5], several design and operating parameters must be optimized such as compression ratio, spark timing, inlet pressure and temperature, and equivalence ratio. This can be achieved through extensive engine testing, but it can be both expensive and time consuming, especially in early design stages. The Interactive Design approach makes use of several techniques to achieve its main goal: supply efficient solutions for leading product engineering [6]. Among them is the use of numerical methods and computational models to address a design problem (like the one mentioned before), with which similar results to those obtained by doing real tests can be achieved. For the design problem addressed in this paper, an engine computational model is a valuable alternative as it can be used to predict pressure and temperature inside engine cylinders, under several initial conditions in a cheap and fast way, and from temperature and pressure profiles, power output, engine efficiency, pollutant emissions, specific fuel consumption and other important engine parameters and indices can be obtained.

An engine model can be zero-dimensional, quasi-dimensional or multi-dimensional [7]. Zero-dimensional and quasi-dimensional models are based on the application of the first law of thermodynamics (energy and mass balances) and ideal gas law on the different stages of the engine cycle namely intake, compression, combustion, expansion and exhaust. Depending on the number of zones considered during the combustion stage in the model, they can be single-zone, two-zones or multi-zones, being the most common the two-zones model where a burned gases zone and an unburned gases zone are considered. While zero-dimensional models use an empirical correlation to predict combustion heat release rate and the development of the flame, quasi-dimensional models do it based on the cylinder dimensions, flame propagation speed and flame geometry. On the other hand, multi-dimensional models are based on the full set of governing partial-differential conservation equations, and so, spatial and temporal information of the cylinder can be obtained from this type of model. However this detail level comes with a substantial increase in the computation time required to solve those equations [8], which makes this model inadequate for parametric studies of the engine.

Knock is an abnormal combustion phenomenon, and its effects range from reduction of the engine efficiency on light knock, to severe engine damage on heavy knock like erosion, holing or melting of cylinder walls [9] and piston surface [10,11]. It occurs when the temperature and pressure of the unburned gas mixture in front of the flame in the cylinder (i.e. end gas) are high enough to promote the increase in the concentration of highly reactive radicals to a critical level in which a portion of this gas undergoes spontaneous chemical reactions known as auto-ignition, releasing most of its chemical energy 5–25 times faster than the normal combustion, causing a sudden substantial increase in temperature and pressure [11]. When increasing inlet pressure with turbocharging, increasing compression ratio or advancing spark timing to increase power output or improve efficiency in natural gas engines, the likelihood of knock occurrence increases [12] and this becomes a constraint in further improvement of SI engines. Hence it is crucial to take into account knock occurrence in engine computational models.

Engine computational models can predict the onset and (to a lesser extent) intensity of knock, modelling it as the

auto-ignition of the end gas, which depends on the temperature and pressure inside the cylinder [13]. There are mainly two models to predict knock onset: the knock integral model and the chemical kinetic model. The knock integral model uses an empirical Arrhenius-like correlation obtained from temperature and pressure measurements in a specific engine, to obtain the ignition delay time τ, the time required for the end gas to attain auto-ignition. This equation is used in the integral equation proposed by Livengood and Wu [14] (Eq. 1) to calculate the time or crank angle degree CAD (θ_{knock}) in which the end gas auto-ignition occurs.

$$\int_{\theta_{IVC}}^{\theta_{knock}} \frac{d\theta}{\tau} = 1 \tag{1}$$

In Eq. 1 θ_{IVC} is the CAD of Intake Valve Close and θ_{knock} is the CAD of knock occurrence. This model was used by [15], using a τ correlation like the one shown in Eq. 2, where p is in-cylinder pressure, T is in-cylinder temperature and X_1, X_2 and X_3, are experimental constants that must be fitted to a specific engine. With this model Soylu [15] was able to predict knock onset with deviations not greater than 0.8 CAD from measured data.

$$\tau = X_1 \cdot p(\theta)^{-X_2} e^{\left(\frac{X_3}{T_u(\theta)}\right)} \tag{2}$$

On the other hand, the chemical kinetic model calculates the knock onset based on a kinetic mechanism (global, reduced or detailed) containing information of the reactions, and transport and thermodynamic properties of a set of species, from which chemical reaction rates can be obtained knowing temperature, pressure and composition of the end gas. Coupled with an engine model, that gives temperature and pressure values at any CAD to the kinetic mechanism, the knock onset can be calculated.

Gao [16] proposed a knock criterion K_c (see Eq. 3) that compares accumulated amount of energy release due to end gas pre-ignition reactions relative to the current volume of the cylinder, with the total energy to be released normally through flame propagation over the whole cycle relative to the swept volume of the cylinder, to detect the knock occurrence. This ratio can be considered as a knock intensity indicator too [17].

$$K_c = \frac{\frac{\text{energy released by end gas reactions } (\theta)}{V(\theta)}}{\frac{\text{energy released by combustion}}{V_d}} \tag{3}$$

This equation was expressed in terms of enthalpies by [17] in Eq. 4 where h_{st} is the air–fuel mixture enthalpy at spark timing (st), $h(\theta)$ is the enthalpy at θ CAD, $m(\theta)$ is the zone (u or b) mass at θ CAD, V_d is the cylinder swept volume, LHV is the lower heating value of the fuel used, m_{fuel} is the fuel mass at spark timing and $V(\theta)$ is the cylinder volume at θ CAD.

$$K_c = \frac{h_{st} \cdot h_u(\theta) \cdot m_u(\theta) \cdot V_d}{LHV \cdot m_{fuel} \cdot V(\theta)} \tag{4}$$

This type of model is more computationally demanding than the knock integral model, and its accuracy depends on the kinetic mechanism used, given that kinetic mechanisms are developed under specific conditions and for a specific range of temperatures and pressures, and should be used with care out of their bounds. Even so, if a suitable mechanism is used, this models can be highly accurate as can be seen in Saikaly et al. [18] where knock occurrence was calculated for several initial conditions and several gas natural compositions, and good agreement was obtained with previous work. Moreover, in Trijselaar [19], experimental knock limited spark time for 8 different natural gas mixtures was obtained and compared to the corresponding knock criterion calculated for every mixture, and it was found as in Saikaly et al. [18], Attar [17,20] that when the knock criterion equals or surpasses a specific value, it can be said that knock occurred.

Heat transfer from the gases to the cylinder walls in the energy balance can account for 30 to 40% of the energies inside the cylinder [21], and therefore, its correct simulation is fundamental for an accurate prediction of the temperature and pressure, and in turn, a correct knock occurrence prediction too. Several correlations like the ones from Eichelberg [22], Woschni [23], Hohenberg [24], Sitkei and Ramanaiah [25] and Annand [26] have been developed to calculate the gas-wall heat transfer coefficient h_g in Newton equation (Eq. 5) for heat transfer rate, where k subscript is either u for unburned air–fuel mixture or b for combustion products. In this equation A_s is the heat transfer area, T_k is the k zone temperature and T_w is the wall temperature.

$$dQ_k = h_{g,k} \cdot A_{s,k} \cdot (T_k - T_w) \tag{5}$$

Lounici et al. [27] tried the five heat transfer correlations mentioned to find the most suitable to predict the in-cylinder pressure, comparing the heat transfer coefficient obtained from each of the correlations, with experimental data, and found that pressure and temperature calculated with the engine model vary considerably depending on the heat transfer correlation used, being Hohenberg's correlation the most suitable for their experimental data. In literature of knock models, the heat transfer coefficient correlations have been used without justification regarding its effect in the knock prediction accuracy. For instance Ghanbari et al. [28], Essen et al. [29] and Gersen et al. [30] used the Woschni correlation, Michos [31] and Soylu [32] used the correlation from Annand and Saikaly et al. [18] used the one from Hohenberg without specifying the reason of their choice. This is why in the cur-

rent study a similar methodology to the one from Lounici is used, but instead of the in-cylinder pressure, K_c is evaluated to determine which one of the correlations predicts better knock occurrence. To calculate K_c, a zero-dimensional two-zone engine model, coupled with a chemical kinetic model for end-gas auto-ignition calculation is used and described. A zero-dimensional model is used because of its simplicity and the lack of experimental turbulence data needed to calibrate a quasi-dimensional model; two zones (urburned and burned) are used during the combustion stage because they are suffice to model knock occurrence, and chemical kinetics model is used instead of the knock integral one because the former takes into account that combustion or oxidation reactions are a sequence of elementary chain reactions with a large number of intermediate species and the latter doesn't.

With the correlation found to be the most suitable to predict K_c, a parametric study is done to evaluate the effect of spark timing, compression ratio, equivalence ratio and inlet temperature in knock occurrence and intensity.

Cantera software [33] was used to calculate the net production rates, the thermodynamic and the transport properties of each species inside the cylinder using the kinetic mechanism developed by Petersen et al. [34] which was found by Trijselaar [19] to be suitable to predict knock in natural gas engines.

The design problem addressed in this work was intended to be solved by means of the interactive design approach, and accordingly the engine computational model was considered as the product meant to solve this problem. According to this approach, the creation of a product is constrained by 3 factors: the expert's knowledge, the realization of functions and the end user's satisfaction [6]. The expert's knowledge was obtained from the engine modeling literature, and was crucial to develop the model described in this work, and the realization of functions is well defined for this model in the last paragraphs. To address the end user's satisfaction a small Application programming interface (API) was developed in the programming language Python, to make use of the model in an interactive way. With this API the user can easily specify the operational and design parameters of the engine, run the engine cycle simulations and plot or process the results. For more information on this API, feel free to contact the authors.

2 Model description

Energy and mass conservation equations, and ideal gas law were applied in every stage of the SI engine cycle, namely Intake stage where the air–fuel mixture enters the cylinder, Compression stage where this mixture is compressed, and pressure and temperature increase, Combustion stage where this mixture is burned and chemical energy stored in the fuel is converted into mechanical energy, and expansion stage

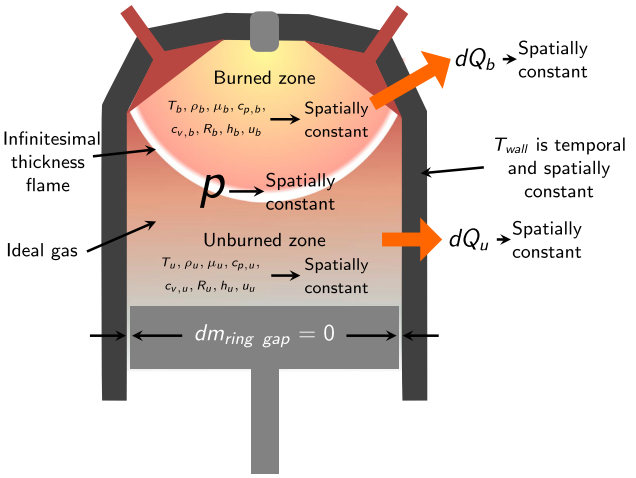

Fig. 1 Schematic diagram of the assumptions made in the SI engine cycle model

where combustion products expand as the piston moves away from the spark plug of the cylinder.

To simplify the SI engine cycle modelling the following assumptions were made: the gases mixture inside the cylinder is an ideal gas; during combustion, cylinder volume is divided in two homogeneous zones, the unburned zone containing the air–fuel-residuals mixture not burned yet and the burned zone containing the products of combustion, separated by an infinitesimal thickness flame; thermodynamic properties are uniform in each zone; total mass of the mixture inside the cylinder is constant during compression, combustion and expansion; pressure in the cylinder is spatially constant since the speed of sound, at which the pressure is equalized, is several orders of magnitude larger than the speed of the flame propagation [13] and Wall temperature is spatially constant. These assumptions are represented in Fig. 1.

Sections 2.1, 2.2 and 2.3 explain the equations obtained for every SI engine cycle stage, and the additional submodels necessary to solve the resulting ordinary differential equation system are described in the remaining subsections.

2.1 Intake process

The present model was developed for port fuel injection engines, as they are more likely to knock than direct injection engines, since in the last ones the charge is cooled when the fuel is injected in the cylinder, because it evaporates using the heat of the charge instead of the heat of the walls, and therefore, knock occurrence likelihood decreases with the charge temperature reduction [35]. In port fuel injection engines the intake process starts at exhaust valve close (EVC) and ends at inlet valve close (IVC). During this process, the intake valve is open and fresh air–fuel mixture enters the cylinder at a rate of dm_{in}. Energy conservation is applied to calcu-

late the change of temperature (Eq. 6), mass conservation is shown in Eq. 7, and pressure change is calculated from ideal gas law (Eq. 8).

$$dT_u = -\frac{dQ_u + p \cdot dV_u + u_u \cdot dm_u - h_{in} \cdot dm_{in}}{m_u \cdot c_{v,u}} \tag{6}$$

$$dm_u = dm_{in} \tag{7}$$

$$dp = p\left(\frac{dT_u}{T_u} + \frac{dm_u}{m_u} - \frac{dV_u}{V_u}\right) \tag{8}$$

In Eq. 6 dQ is the heat transfer rate, h_{in} is the intake mixture enthalpy and c_v is the specific heat capacity at constant volume. To calculate dm_{in} the equations for compressible flow through a flow restriction shown in Eqs. 9 and 10 are used [11]. Flow area of the valve (A_R) is calculated with Eq. 11 and p_T, p_o and T_o are calculated with Eq. 12. In this equation subscript in corresponds to intake mixture properties. If $\frac{p_T}{p_o} \leq \left(\frac{2}{\gamma+1}\right)^{\frac{\gamma}{\gamma-1}}$ is true, Eq. 10 is used instead of Eq. 9.

$$dm_{in} = s\frac{C_D \cdot A_R \cdot p_o}{(R \cdot T_o)^{1/2}}\left(\frac{p_T}{p_o}\right)^{\frac{1}{\gamma}}\sqrt{\frac{2\gamma}{\gamma-1}\left(1-\left(\frac{p_T}{p_o}\right)^{\frac{\gamma-1}{\gamma}}\right)} \tag{9}$$

$$dm_{in} = s\frac{C_D \cdot A_R \cdot p_o}{(R \cdot T_o)^{1/2}}\gamma^{1/2}\left(\frac{2}{\gamma+1}\right)^{\frac{\gamma+1}{2(\gamma-1)}} \tag{10}$$

$$A_R = \pi \cdot D_v \cdot l_{v,max} \cdot \sin\left(\pi\frac{\theta-\theta_{IVO}}{\theta_{IVC}-\theta_{IVO}}\right) \tag{11}$$

$$\begin{cases} p_o = p_{in},\ p_T = p,\ T_o = T_{in},\ s = 1, & \text{for } p_{in} > p \\ p_o = p,\ p_T = p_{in},\ T_o = T_u,\ s = -1, & \text{for } p_{in} < p \end{cases} \tag{12}$$

In Eqs. 9, 10 and 11 C_D is the discharge coefficient of intake valve, R is the specific gas constant, γ is the specific heat capacities ratio, D_v is the intake valve diameter and $l_{v,max}$ is the maximum intake valve lift.

2.2 Compression and expansion processes

Compression starts at IVC and ends at spark timing (ST), while expansion starts at the end of combustion and ends at exhaust valve open (EVO). Same differential equations were obtained for both processes. Using energy and ideal gas law, Eqs. 13 and 14 are obtained respectively.

$$dT_k = -\frac{dQ_k + p \cdot dV_k}{m_k \cdot c_{v,k}} \tag{13}$$

$$dp = p\left(\frac{dT_k}{T_k} - \frac{dV_k}{V_k}\right) \tag{14}$$

where subscript k is u (unburned) for compression and b (burned) for expansion.

2.3 Combustion process

Combustion starts at the end of the ignition lag, almost immediately after the spark timing and is considered to end when unburned mixture is 95% of the total mass in the cylinder. Ignition lag is calculated with an empirical correlation (Eq. 15) obtained by Rousseau et al. [36] where ϕ is the equivalence ratio.

$$\theta_{lag} = -0.35\theta_{st} + 6.80/\phi - 3.848 \tag{15}$$

The initial burned zone temperature and the initial composition of the burned zone are assumed to be the adiabatic flame temperature and equilibrium composition respectively of the unburned mixture at spark timing, obtained from equilibrium calculation carried out adiabatically and at constant pressure. Both are obtained using the Gibbs energy minimization method included in Cantera.

Energy conservation was applied in both zones, unburned (Eq. 16) and burned (Eq. 17) and ideal gas law was used to calculate p evolution (Eq. 18). The composition of both zones is considered transient and dependent on the chemical reactions occurring in each one. Equations to calculate this change are Eqs. 19 and 20 for unburned and burned zones respectively and the energy contribution of this reactions, $dQ_{chem,u}$ and $dQ_{chem,b}$ (Eqs. 21 and 22), is included in the energy conservation equations. This allows to account for possible auto-ignition occurrence in the unburned zone, and thus predict the knock occurrence using the K_c.

$$dT_u = \frac{V_u \cdot dp + dQ_{chem,u} - dQ_u}{m_u \cdot c_{p,u}} \tag{16}$$

$$dT_b = \frac{V_b \cdot dp + dQ_{chem,b} - dQ_b + (h_u - h_b)dm_b}{m_u \cdot c_{p,u}} \tag{17}$$

$$dp = \frac{\begin{array}{l}(-c_{p,b} \cdot R_b \cdot T_b + c_{p,b} \cdot R_u \cdot T_u + R_b \cdot h_b \\ - R_b \cdot h_u)c_{p,u} \cdot dm_b + c_{p,b} \cdot c_{p,u} \cdot p \cdot dV \\ + c_{p,b} \cdot R_u \cdot dQ_u + c_{p,u} \cdot R_b \cdot dQ_b \\ - c_{p,b} \cdot R_u \cdot dQ_{chem,u} - c_{p,u} \cdot R_b \cdot dQ_{chem,b}\end{array}}{-c_{p,b} \cdot c_{p,u} \cdot V + c_{p,b} \cdot R_u \cdot V_u + c_{p,u} \cdot R_b \cdot V_b} \tag{18}$$

$$dY_{i,u} = \frac{M_{i,u} \cdot \omega_{i,u}}{\rho_u} \tag{19}$$

$$dY_{i,b} = \frac{M_{i,b} \cdot \omega_{i,b}}{\rho_b} \tag{20}$$

$$dQ_{chem,u} = -V_u \sum_{i=1}^{N} \tilde{h}_{i,u} \cdot \omega_{i,u} \tag{21}$$

$$dQ_{chem,b} = -V_b \sum_{i=1}^{N} \tilde{h}_{i,b} \cdot \omega_{i,b} \tag{22}$$

In Eqs. 16–22 c_p is the specific heat capacity at constant pressure, ρ_k is the k zone density, and $\tilde{h}_i$, M_i and ω_i are the partial molar enthalpy, molecular mass and net production rate of species i respectively.

2.4 Cylinder volume

Volume inside the cylinder is calculated with Eq. 23, where V_c is the cylinder clearance volume, B is the cylinder bore, S is the cylinder stroke length and L is the connecting rod length.

$$V = V_c + \frac{\pi \cdot B^2}{4}\left(L + \frac{S}{2}\left(1 - \cos(\theta) - \sqrt{L^2 - \frac{S^2}{4}\sin^2(\theta)}\right)\right) \tag{23}$$

2.5 Combustion heat release rate

The mass burning rate dm_b in the combustion equations is related to the combustion heat release rate (dQ_r) through the LHV ($dm_b = dQ_r/LHV$). The analytical equation for dQ_r proposed by [37] which takes into account the turbulence inside the cylinder through constant C_T is used. Equation 24 shows this model, where t' is the time elapsed since spark ignition and x_b is the burned mass fraction.

$$dm_b = C_T \cdot \rho_b \cdot s_L \cdot t'^2(1 - x_b) \tag{24}$$

s_L can be obtained from a free flame model, experimentally or with correlations. In the current work s_L was calculated for temperatures from 300 to 900 K, pressures from 1 to 90 bar and equivalence ratios from 0.6 to 1.1 with the free flame model from Cantera and through data fitting a multivariate polynomial was obtained for s_L as a function of these three parameters.

2.6 Knock occurrence

Derivative of K_c (Eq. 25) is solved along with the other differential equations in the combustion stage to get K_c evolution in time, and it is considered that knock occurs when K_c is equal or greater than 1.5, from the results obtained by Attar [17] who found that borderline knock is found when the maximum value reached by K_c is the mentioned value. In Eq. 25 CR is the compression ratio.

$$\begin{aligned} dK_c = \frac{1}{V}(V_c \cdot CR((h_{st} - h_u)dm_b \\ + m_u \cdot c_{p,u} \cdot dT_u)/LHV - K_c \cdot dV) \end{aligned} \tag{25}$$

2.7 Heat transfer model

Five heat transfer coefficient correlations are compared to find the most suitable to predict the knock occurrence. Equation 26 is the correlation from Woschni [23], Eq. 27 comes from Eichelberg [22], Eq. 28 is the one from [26], Eq. 29 corresponds to Hohenberg [24] and Eq. 30 to Sitkei and Ramanaiah [25]. In these equations s_p is the averaged piston speed and units of measurement are those of the International System of Units (SI), unless otherwise specified.

$$h_g = 129.8 \cdot B^{-0.2}(p[\text{bar}] \cdot w)^{0.8} \cdot T^{-0.53} \tag{26}$$

$$h_g = 7.67 \times 10^{-3} s_p^{1/3}(p \cdot T)^{0.5} \tag{27}$$

$$h_g = a\frac{k_g}{B}\left(\frac{s_p \cdot B \cdot m}{V \cdot \mu}\right)^{0.7} + 4.3 \times 10^{-9}\frac{T^4 - T_w^4}{T - T_w} \tag{28}$$

$$h_g = 130V^{-0.06}p[\text{bar}]^{0.8}T^{-0.4}(1.4 + s_p)^{0.8} \tag{29}$$

$$h_g = 2.36 \times 10^{-4}(1 + b)\frac{(p \cdot s_p)^{0.7}A_s^{0.3}}{T^{0.2}(4V)^{0.3}} \tag{30}$$

In correlation from Woschni Woschni (Eq. 26), w is the gas velocity, calculated from the unfired gas velocity (proportional to the averaged piston speed) and the combustion induced gas velocity (function of the difference between the motoring and firing pressures) [27], and is calculated with Eq. 31, where the subscript st means "at spark timing"; and p_{mot}, the motoring pressure, is calculated with Eq. 32. Moreover, Woschni found that C_1 is 6.18 in intake and 2.28 in compression, combustion and expansion; and C_2 is 0 in intake and compression and 3.24×10^{-3} in combustion and expansion.

Constant a in Eq. 28 from Annand and constant b in Eq. 30 from Sitkei and Ramanaiah are tuning parameters with ranges of 0–0.35 and 0.35–0.8 respectively. The values of these parameters were chosen in order to obtain the results closest to the experimental data used.

$$w = C_1 \cdot s_p + C_2(p - p_{mot})\frac{V_d \cdot T_{st}}{p_{st} \cdot V_{st}} \tag{31}$$

$$p_{mot} = p_{st}\left(\frac{V_{st}}{V}\right)^{1.3} \tag{32}$$

In the Newton's equation (Eq. 5) the A_s for intake, compression and expansion is calculated with Eq. 33 [11]. $A_{s,b}$ and $A_{s,u}$ during combustion are obtained from Eqs. 34 and 35 respectively [27].

$$A_s = \pi/(2B^2) + 4V/B \tag{33}$$

$$A_{s,b} = A_s\sqrt{x_b} \tag{34}$$

$$A_{s,u} = A_s - A_{s,b} \tag{35}$$

Table 1 Design and operating conditions of studied engines

	B (mm)	S (mm)	rpm	CR	p_{in} (bar)	Fuel	ST (CAD)	ϕ
Attar	82.5	114	900	8.5	0.87	CH_4	10	0.9
Saikaly	152	165	1500	12	1.6	Natural gas	14	0.69

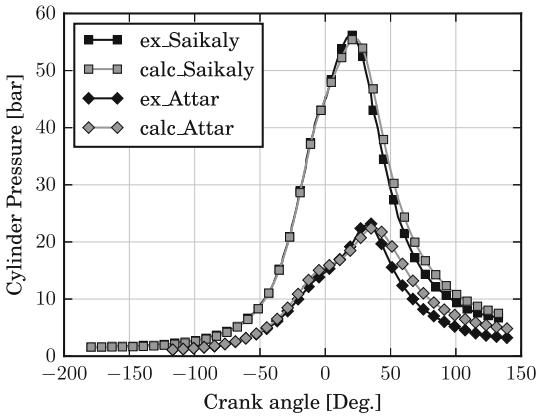

Fig. 2 Experimental and calculated cylinder pressure for studied engines

2.8 Engine model solving

To solve the ordinary differential equations system obtained from the equations previously explained, the *ode* solver from python library Scipy [38] was used, with a method based on backward differentiation formulas (BDF) for stiff problems, due to the high stiffness of the set of ordinary differential equations obtained from Eqs. 19, 20, 21 and 22.

3 Results and discussion

3.1 Model validation

Pressure inside the cylinder was chosen as the comparison criterion for overall model validation since, from this parameter, the performance of an engine can be evaluated. Experimental pressure data from Attar [17] and Saikaly et al. [39] was used to test the performance of the current model at different design and operating conditions (see Table 1), and results are shown in Fig. 2 where "ex" means experimental data and "calc" calculated data.

The C_T constant in Eq. 24 was adjusted to fit the experimental data using the least squares method. The peak pressure and the peak pressure CAD predicted by the model, were close to the experimental data for Saikaly and this was checked with the Mann–Whitney U test [40], a statistical test to find if two data set's difference is significant, with which it was found that difference between experimental and calculated data is not significant. On the other hand the model predicted a peak pressure slightly smaller than the experimental peak pressure for Attar but the peak pressure CAD for the model is approximately equal in both experimental and calculated data. Mann–Whitney U test applied to compare experimental and calculated data resulted in the difference between the two being significant, due to the overestimation of pressure during expansion stage. However, this difference is not significant for the current work since the interest is in knock prediction and knock occurs during combustion stage and during this stage pressure prediction was accurate.

Considering that the model used is zero-dimensional and a lot of assumptions were made to simplify the SI engine modelling, the results obtained are satisfactory. Nonetheless, it is important to compare not only the pressure, but also the K_c to determine if the current model is able to predict knock occurrence, since this parameter has been found to be associated directly with the end-gas autoignition.

Table 2 Design and operating conditions where it was found by [17] that knock occurred

Test	1	2	3	4	5	6	7	8
ϕ	1.00	0.77	0.83	0.94	0.90	0.90	0.90	0.90
CR	11	16	15	14	16	15	14	12
ST	28.00	17.00	17.00	17.00	12.74	14.91	17.70	24.32

3.2 Heat transfer model influence on Knock

Attar [17] found several engine design and operating conditions where knock occurred, varying compression ratio, equivalence ratio, spark timing and initial temperature. At these conditions the maximum value of the K_c ($K_{c,max}$) was close to 1.5. Some of these design and operating conditions are shown in Table 2 and are used in conjunction with the engine specifications of Attar (see Table 1) to calculate the $K_{c,max}$ using the five correlations mentioned in Sect. 2.7.

Figure 3a shows the $K_{c,max}$ of every test shown in Table 2 calculated with the different heat transfer coefficient correlations, and Fig. 3b shows the difference between the $K_{c,max}$ calculated and the reference value 1.5 ($\Delta K_{c,max} = |K_{c,max} - 1.5|$).

In Fig. 3a it can be seen that $K_{c,max}$ calculated with Annand and Sitkei correlations are closer to 1.5 than those from Woschni, Eichelberg and Hohenberg, and this is confirmed in Fig. 3b where $\Delta K_{c,max}$ in the first correlations is not greater than 0.5 and are far lower than the other corre-

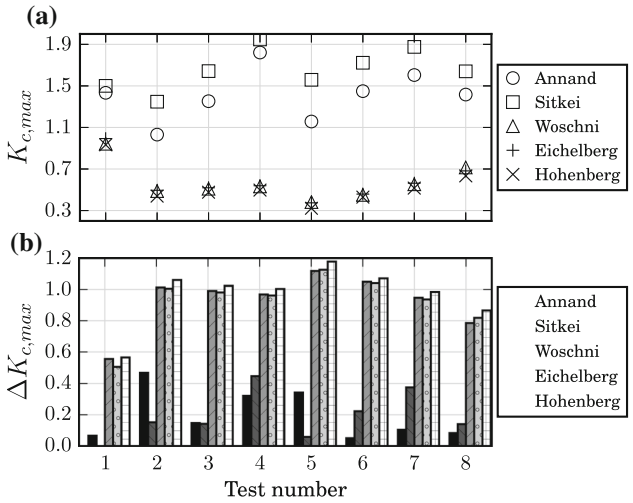

Fig. 3 **a** $K_{c,max}$ of tests in Table 2, **b** $\Delta K_{c,max}$

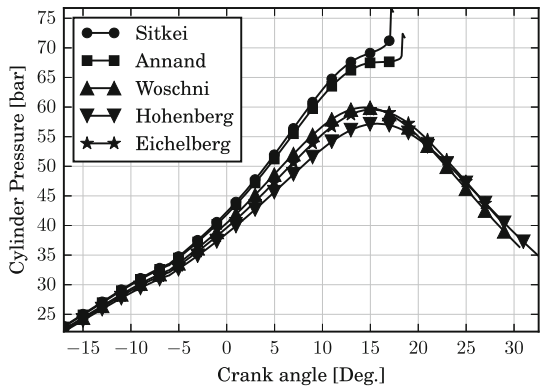

Fig. 4 In-cylinder pressure calculated for test 2 with the five heat transfer correlations

lations. It was also found that with the Woschni, Hohenberg and Eichelberg correlations no knock was detected in most of the tests, whereas with the Annand and Sitkei correlations, knock was detected in all of the tests, which is in agreement with what was reported by Attar. This can be seen in Fig. 4 where in-cylinder pressure calculated for test 2 with the five correlations is shown. In this figure the curves from Sitkei and Annand have a sudden rise in pressure, indicative of knock, and the others don't exhibit this behaviour.

In tests 1, 2, 3 and 5 Sitkei's correlation performed better since $\Delta K_{c,max}$ was the smallest of the five correlations, while in the other four tests the correlation from Annand was better. Sitkei's correlation seems to overestimate $K_{c,max}$ and Annand seems to underestimate it, given that their means were 1.65 and 1.4 respectively, but more data would be required to make such a conclusion. On the other hand, although just in test 1 the $K_{c,max}$ is equal to 1.5 (with Sitkei), in all of the tests these two correlations detected the knock and with values of $K_{c,max}$ close to 1.5, and therefore, both equations are able to predict the occurrence of knock for the experimental data used. This same methodology can be applied for different engines to find the most suitable heat transfer coefficient correlation in order to predict as accurately as possible knock occurrence when certain design and operating parameters are used.

3.3 Knock occurrence

A parametric analysis was performed to study the effect of spark timing (ST), compression ratio (CR), equivalence ratio (ϕ) and inlet temperature (T_{in}) on knock occurrence for a natural gas engine like the one studied by Attar (see Table 1). Design and operating conditions used in the study include $CR = 13$, $ST = 18$ CAD BTC and $\phi = 0.8$, and the remaining parameters are those given in Table 1 for Attar engine. Knock does not occur at these conditions, and therefore they were chosen as the starting point for the parametric study. To study one variable the other ones are held constant while the one studied is given several values that go from non-knocking to knocking conditions. The calculation time to execute the simulation of the engine model with the Sitkei correlation was smaller than that of Annand and, therefore, the first one was used in the parametric study.

Spark timing has a substantial effect in knock occurrence, and is the most commonly changed parameter to avoid it. Knock increases when spark timing is advanced because the greater the spark advance, the longer the combustion takes place in the compression stage, where the pressure and temperature are increasing and therefore there is a greater probability of knock occurring. Taking into account the above, spark timing was advanced from 18 CAD until knock was detected, with intervals of 3 CAD. Results are shown in Fig. 5 where p versus CAD is plotted. The sudden increase in pressure indicates knock onset, and difference between pressure after and before knock onset gives a notion of its intensity. Results are consistent with theory just explained, and the greater the spark advance is, the sooner knock occurs and the higher the knock intensity is.

In SI engines there is a trade-off between knock avoidance and engine efficiency or power output, since higher temperature and pressure are reached when compression ratio is increased and therefore, likeability of knock increases too, but with greater compression ratio a higher efficiency is attained and more air–fuel mixture enters the cylinders, with more power output as a result. It is important therefore to find the knock limited compression ratio for given operating conditions and take this into account to design the engine. With an engine model a starting point to the design process can be found using a method like the one applied in the present work in which compression ratio was increased from non-knocking compression ratio at 13, until knock was detected at compression ratio of 16. Results are shown in

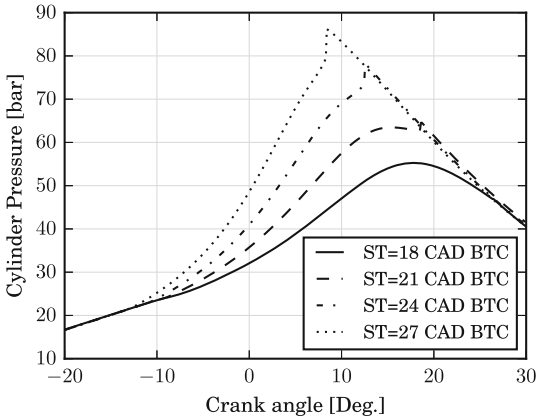

Fig. 5 Knock onset and intensity when varying spark timing

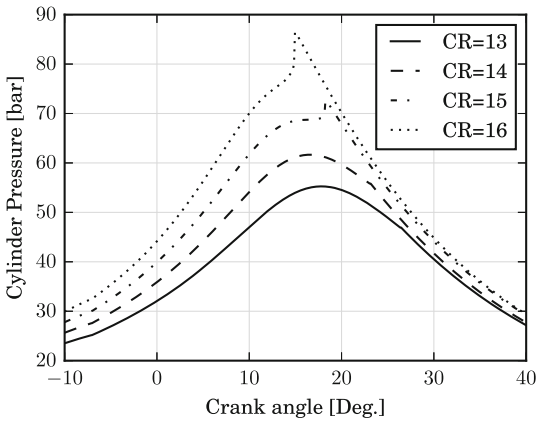

Fig. 6 Knock onset and intensity when varying compression ratio

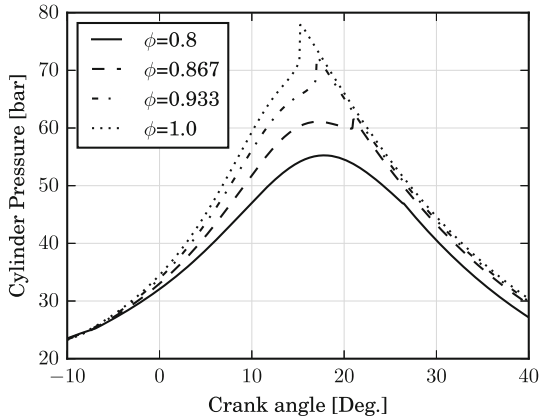

Fig. 7 Knock onset and intensity when varying equivalence ratio

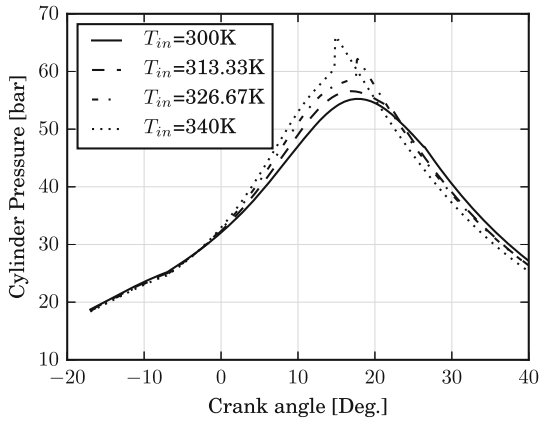

Fig. 8 Knock onset and intensity when varying inlet temperature

Fig. 6 and as predicted, knock occurred when the compression ratio reached a sufficiently high value.

When the equivalence ratio approaches 1, stoichiometric combustion is reached, and the maximum amount of fuel and air is consumed during the reaction, whereby the maximum amount of energy is released during combustion as compared to poor or rich combustion. However, in this condition the temperature increases and so does the probability of knock. This can be seen in Fig. 7, where knock intensity is greater at $\phi = 1$.

Turbocharging increases inlet pressure, so more air–fuel mixture enters the cylinders and more energy is obtained from combustion. One drawback of this technology is the inlet temperature rise, which as has been stated before promotes knock occurrence. It is important to find then how much can the inlet temperature increase in a natural gas engine to get higher power output, without reaching knock conditions, and to get an estimate of this condition inlet temperature in the engine model was increased until knock was found. As can be seen in Fig. 8 inlet temperature increase of just 40 K from ambient conditions is sufficient to trigger knock.

As it is confirmed with this parametric study, the current model is in accordance with theory about behaviour of knock occurrence when spark timing, compression ratio, equivalence ratio and inlet temperature are varied.

4 Conclusions

Developed zero-dimensional two-zones model was validated against experimental data, and used to predict knock occurrence through calculation of $K_{c,max}$. To predict knock as accurate as possible five heat transfer coefficient correlations were used in the model and the $K_{c,max}$ values calculated with each of them at different design and operating conditions were compared to find the most suitable to knock occurrence prediction. It was found that for the experimental knock data used the best correlations were those from Sitkei [25] and Annand [26]. This same methodology can be applied for different engines to find the most suitable heat transfer coefficient correlation in order to predict as accurate as possible knock occurrence when certain design and operating parameters are considered. A parametric analysis

was made to study the effect of spark timing, compression ratio, equivalence ratio and inlet temperature on knock occurrence and test if the model is coherent with real engine knock behaviour. Results of this study show that model predicts well knock occurrence likelihood increase when spark timing is advanced, compression ratio is higher, equivalence ratio is closer to 1 and initial temperature is greater. The parametric method described can be used to decide which parameters can be changed to avoid knock occurrence, both during engine design with spark timing, compression ratio and inlet temperature, and during engine operation with equivalence ratio and inlet temperature. Further research is needed to determine which parameter is the most suitable to be varied when considering certain conditions, taking into account the emissions, the specific fuel consumption and the power output variation when each of them is changed.

References

1. Gao, P., Kaas, H.W., Mohr, D.: Automotive revolution: perspective towards 2030. McKinsey & Company, Technical Report (2016)
2. The Environmental Protection Agency (EPA), Clean alternative fuels: Compressed natural gas, fact sheet, (2002)
3. Korakianitis, T., Namasivayam, A., Crookes, R.: Natural-gas fueled spark-ignition (SI) and compression-ignition (CI) engine performance and emissions. Prog. Energy Combust. Sci. **37**(1), 89–112 (2011)
4. Clean Cities, Clean cities alternative fuel price report. U.S. Department of Energy, Technical Report (2017)
5. Chica, J.A.V., Torres, A.G.D., Acosta, D.A.: NMPC controller applied to the operation of an internal combustion engine: formulation and solution of the optimization problem in real time. In: International Journal on Interactive Design and Manufacturing (IJIDeM) (2016)
6. Fischer, X.: Research in Interactive Design Vol. 3: Virtual, Interactive and Integrated Product Design and Manufacturing for Industrial Innovation. Springer, Berlin (2010)
7. Medina, A., Curto-Risso, P., Calvo, A., Guzmán-Vargas, L., Angulo-Brown, F., Sen, A.: Quasi-Dimensional Simulation of Spark Ignition Engines. Springer, Berlin (2014)
8. Caton, J.A.: An Introduction to Thermodynamic Cycle Simulations for Internal Combustion Engines. Wiley, Chichester (2015)
9. Lee, W., Schaefer, H.J.: Analysis of local pressures, surface temperatures and engine damages under knock conditions. In: SAE International Congress and Exposition, 1983. SAE International (1983)
10. Fitton, J., Nates, R.: Knock erosion in sparkignition engines. In: 1996 SAE International Fall Fuels and Lubricants Meeting and Exhibition. SAE International (1996)
11. Heywood, J.: Internal Combustion Engine Fundamentals. McGraw-Hill Education, New York (1988)
12. Chen, L., Li, T., Yin, T., Zheng, B.: A predictive model for knock onset in spark-ignition engines with cooled EGR. Energy Convers. Manag. **87**, 946–955 (2014)
13. Guzzella, L., Onder, C.H.: Introduction to Modeling and Control of Internal Combustion Engine Systems. Springer, Berlin (2010)
14. Livengood, J., Wu, P.: Correlation of autoignition phenomena in internal combustion engines and rapid compression machines. In: Symposium (International) on Combustion, vol. 5, no. 1, pp. 347–356 (1955)
15. Soylu, S.: Prediction of knock limited operating conditions of a natural gas engine. Energy Convers. Manag. **46**(1), 121–138 (2005)
16. Gao, J.: Knock modeling in s.i. engines. Ph.D. thesis, Department of Mechanical Engineering, University of Calgary (1993)
17. Attar, A.A.: Optimization and knock modeling of a gas fueled spark ignition engine. Ph.D. thesis, University of Calgary, Ottawa (1997)
18. Saikaly, K., Rousseau, S., Rahmouni, C., Corre, O.L., Truffet, L.: Safe operating conditions determination for stationary SI gas engines. Fuel Process. Technol. **89**(11), 1169–1179 (2008)
19. Trijselaar, A.: Knock prediction in gas-fred reciprocating engines. Master's thesis, University of Twente, Enschede, The Netherlands (2012)
20. Karim, G.A., Gao, J.: Developing a knock predictive criterion in spark ignition engines fuelled with gaseous fuels. J. Therm. Sci. **2**(4), 304–311 (1993)
21. Guibert, P.: Modélisation du cycle moteur approche zérodimensionnelle, Techniques de l'ingénieur. Génie mécanique, no. BM2510 (2005)
22. Eichelberg, G.: Some new investigations on old combustion engine problems. Engineering **148**(27), 463–466 (1939)
23. Woschni, G.: A universally applicable equation for the instantaneous heat transfer coefficient in the internal combustion engine. Technical Report, SAE Technical paper (1967)
24. Hohenberg, G.F.: Advanced approaches for heat transfer calculations. In: 1979 SAE International Off-Highway and Powerplant Congress and Exposition. SAE International (1979)
25. Sitkei, G., Ramanaiah, G.V.: A rational approach for calculation of heat transfer in diesel engines. In: 1972 Automotive Engineering Congress and Exposition. SAE International (1972)
26. Annand, W.J.D.: Heat transfer in the cylinders of reciprocating internal combustion engines. Proc. Inst. Mech. Eng. **177**(1963), 973–996 (1963)
27. Lounici, M.S., Loubar, K., Balistrou, M., Tazerout, M.: Investigation on heat transfer evaluation for a more efficient two-zone combustion model in the case of natural gas SI engines. Appl. Therm. Eng. **31**(2–3), 319–328 (2011)
28. Ghanbari, M., Safari, H., Jazayeri, S.A., Ebrahimi, R.: A refined analytical combustion model for evaluating the effects of EGR percentage on improvement of knock characteristics of natural gas in spark ignition engine. In: Volume 3: Combustion Science and Engineering, vol. 3, pp. 45–54. ASME International (2008)
29. Essen, M.V., Gersen, S., Dijk, G.V., Levinsky, H.: Two-zone thermodynamic model to predict temporal variations in pressure of the end gas in an engine cylinder cycle. In: SAE Technical Paper Series, vol. 6. SAE International (2013)
30. Gersen, S., van Essen, M., Levinsky, H., van Dijk, G.: Characterizing gaseous fuels for their knock resistance based on the chemical and physical properties of the fuel. SAE Int. J. Fuels Lubr. **9**(1), 1–13 (2016)
31. Rakopoulos, C., Michos, C.: Development and validation of a multi-zone combustion model for performance and nitric oxide formation in syngas fueled spark ignition engine. Energy Convers. Manag. **49**(10), 2924–2938 (2008)
32. Soylu, S.: Development of an autoignition submodel for natural gas engines. Fuel **82**(14), 1699–1707 (2003)
33. Goodwin, D.G., Moffat, H.K., Speth, R.L.: Cantera: an object-oriented software toolkit for chemical kinetics, thermodynamics, and transport processes. Version 2.3.0 (2017)
34. Petersen, E.L., Kalitan, D.M., Simmons, S., Bourque, G., Curran, H.J., Simmie, J.M.: Methane/ propane oxidation at high pressures: experimental and detailed chemical kinetic modeling. Proc. Combust. Inst. **31**(1), 447–454 (2007)
35. Kasseris, E., Heywood, J.B.: Charge cooling effects on knock limits in SI DI engines using gasoline/ ethanol blends: part 2-effective octane numbers. SAE Int. J. Fuels Lubr. **5**(2), 844–854 (2012)

36. Rousseau, S., Lemoult, B., Tazerout, M.: Combustion characterization of natural gas in a lean burn spark-ignition engine. In: Proceedings of the Institution of Mechanical Engineers. Part D 32, vol. 213, no. 5, pp. 481–489 (1999)
37. Chmela, F., Engelmayer, R., Beran, R., Ludu, A.: Prediction of heat release rate and NOx emission for large open chamber engines with spark ignition. In: 3rd Dessau Gas Engine Conference (2003)
38. Jones, E., Oliphant, T., Peterson, P., et al.: SciPy: open source scientific tools for Python (2001). https://www.scipy.org/citing.html. Accessed 12 Mar 2017
39. Saikaly, K., Corre, O.L, Rahmouni, C., Truffet, L.: Normalized knock indicator for natural gas s.i. engines: methane number requirements prediction. In: ASME 2009 Internal Combustion Engine Division Fall Technical Conference. ASME International (2009)
40. Mann, H.B., Whitney, D.R.: On a test of whether one of two random variables is stochastically larger than the other. Ann. Math. Stat. **18**(1), 50–60 (1947)